Hindawi
Modelling and Simulation in Engineering
Volume 2017, Article ID 6171303, 10 pages
https://doi.org/10.1155/2017/6171303

Research Article

Numerical Simulation of Magnetic Field Effect on Cryocooler Regenerators: Temperature Distribution

Rajendra Kumar and Sumit Shoor

School of Mechanical Engineering, Lovely Professional University, Phagwara, Punjab 144411, India

Correspondence should be addressed to Rajendra Kumar; rajwithn25@gmail.com

Received 3 August 2016; Revised 6 November 2016; Accepted 21 November 2016; Published 3 January 2017

Academic Editor: Dimitrios E. Manolakos

Regenerative types of cryogenic refrigerators (or cryocoolers) employ magnetic intermetallic compounds of 3d and 4f elements to work well below 10 K. This paper presents the analysis of temperature distribution in regenerators of such cryocoolers under the influence of magnetic fields of 1 T, 3 T, and 4.3 T. Commercial code of finite element analysis (FEA) package, ANSYS (APDL) 14.5, is used to investigate the temperature distribution under above-mentioned fields. Er_3Ni is selected as regenerator material and the criteria for its selection are discussed in detail. The cold end temperature is varied from 4.2 K to 10 K and hot end temperature is fixed at 20 K. The values obtained from FEA clearly show that the ineffectiveness of Er_3Ni is at 8 K and 10 K at 3 T and 4.3 T.

1. Introduction

Cryocoolers are the devices capable of producing temperatures of 120 K and below [1]. Cryocoolers operating with a regenerative type of heat exchanger (regenerators) are known as regenerative cryocoolers and are mainly of three types [2]:

(i) Stirling; (ii) Gifford-McMahon (GM) (Figure 1); and (iii) pulse tube cryocooler (PTC).

The use of magnetic intermetallic compounds in regenerators of cryocoolers improved its functioning below 10 K [3, 4] and liquid He temperatures were reached [5, 6]. The heat capacity of Pb decreases drastically whereas peak in specific heat is observed in such materials below 10 K [7–9].

Figure 2 represents the materials used for different temperature ranges in regenerators along with their geometry. Nowadays cryocoolers are extensively used to cool MRI systems and magnetometers (SQUIDs) where they are continuously exposed to very high magnetic fields ~5 T or even more. Along with magnetic interference, an additional thermal load is also present when electrical resistivity of the material is taken into account.

This paper presents the results of coupled (magnetic + thermal) analysis of cryocoolers regenerator under magnetic field (1 T, 3 T, and 4.3 T) using commercial FEA package, ANSYS (APDL) 14.5. The electrical resistivity of Er_3Ni is also included in the material properties to account for Joule heating. The criteria for selection of Er_3Ni in numerical simulation are discussed. The model shows the ineffectiveness of Er_3Ni above 6 K as well as 1 T.

2. Matrix Material Selection

Till date, various materials have been used for 4 K class of cryocoolers. References [7–9] present few of such materials. The text by Spichkin and Tishin [10] also vastly covers such materials along with their magnetic properties. As seen from [3–10] the most prominent materials used are Er_3Ni, ErNi, $HoCu_2$, and ErPr.

The data present in the literature about the magnetic properties and electrical properties are very limited for cryocooler regenerator materials. While performing a magnetic analysis proper data of magnetic properties must be present. However, regenerator materials are not often described with their magnetic, thermal, and electrical properties simultaneously. All these properties are highly nonlinear at cryogenic temperatures. Therefore, criteria used for selection of regenerator material are summarized as follows:

(i) The material should show variable heat capacity in the temperature ranges below 15 K under magnetic

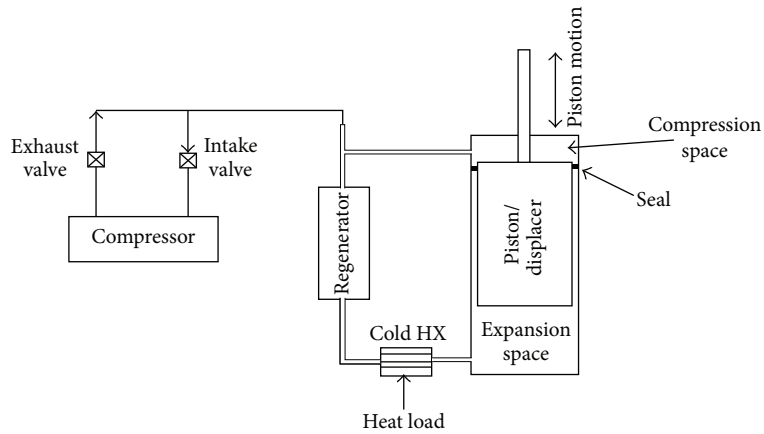

Figure 1: Schematic of GM cryocooler.

Table 1: Material properties of Er_3Ni for ANSYS.

Sr. number	Material properties	Value/nature	References
1	Relative permeability	*1.3* (assumed linear and constant)	[11, 12]
2	Electrical resistivity	Temperature dependent	[13]
3	Néel temperature (T_N)	*7.7 K*	[14]
4	Density	*9290 kg/m*^{3}	[14]
5	Thermal conductivity	*2 W/m K at 50 K* *0.3 W/m K 5 K*	[15]
6	Specific heat under magnetic field	Temperature and magnetic field dependent	[16]

field. Most of the time this temperature is determined by the Curie temperature (T_{curie}) in the case of paramagnetic materials whereas it is determined by Néel temperature (T_N) for antiferromagnetic materials (AFM).

(ii) T_{curie} or T_N for the material should lie below 15 K.

(iii) There are many materials available to use in the regenerator of 4 K cryocoolers. However, the materials may not be readily available as per requirement. Therefore, commercially available materials should be selected.

(iv) The relative permeability is highly nonlinear and must be found experimentally always. Therefore selecting the material whose relative permeability is already present in the literature is necessary. Er_3Ni is the only material whose relative permeability is present as it is.

Table 1 presents the electrical, thermal, and magnetic properties of Er_3Ni from different references that made input to ANSYS. Key points (i)–(iv) are justified after observing Table 1.

Reference [16] is the only work present till date to account for the influence of magnetic field upon the direct values of specific heat for Er_3Ni.

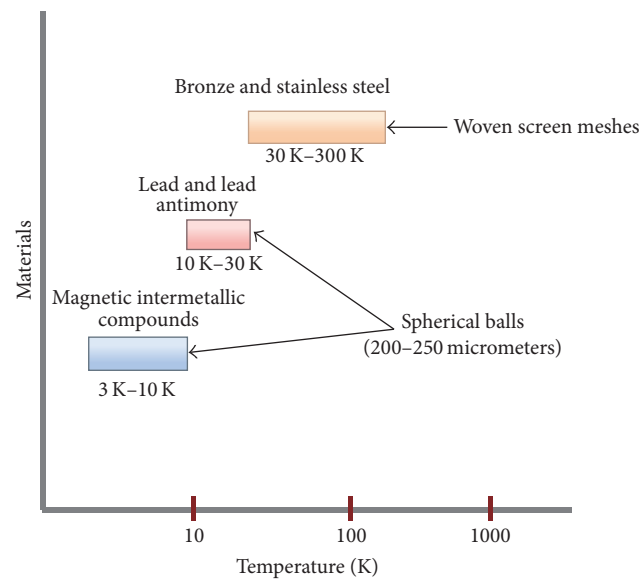

Figure 2: Temperature ranges for regenerator materials used in cryocoolers.

3. Finite Element Modelling in ANSYS

The following subsections describe the various steps for modelling the regenerator with optimal dimensions. The loads, operating conditions, and element selected for analysis are discussed.

3.1. Solid Model. The regenerator considered is 100 mm in length and 20 mm wide. A 2D axisymmetric model with nonuniform magnetic field is considered.

The nonuniform magnetic field is simulated by putting a solenoid/coil in the vicinity of the regenerator. Figure 3 shows the solid model used for simulation.

3.2. Element Selection. Plane13 (vector quad 13) element is selected for the analysis [17]. It allows for 2D thermal, magnetic, and electrical field calculations with limited coupling

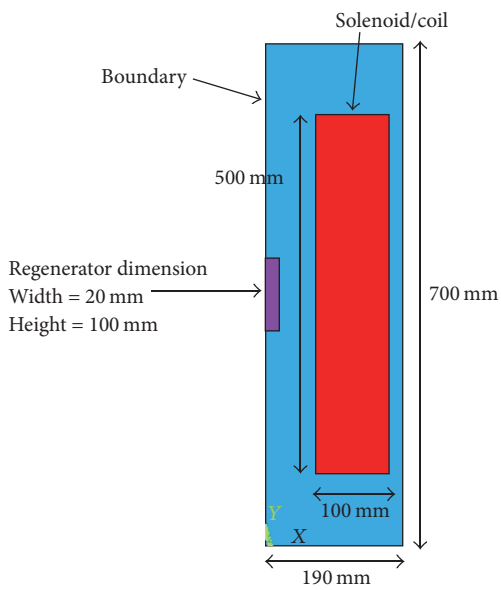

Figure 3: Solid model for simulation in ANSYS.

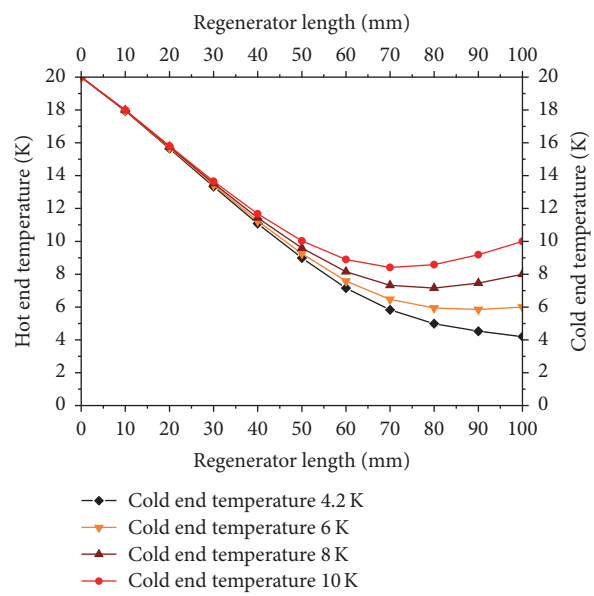

Figure 5: Temperature profile of model at $B = 0$ T.

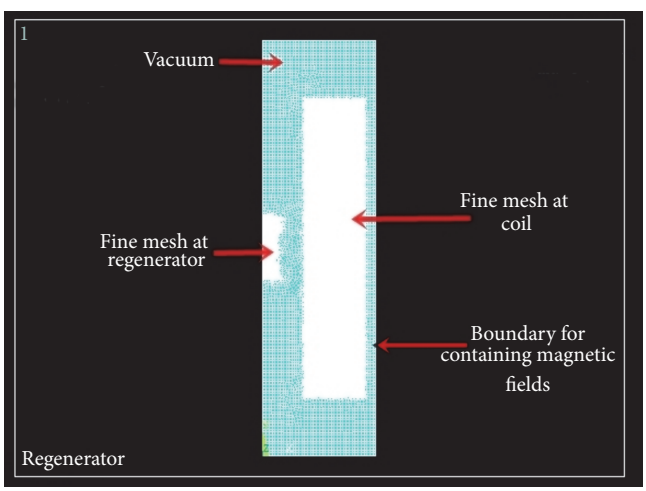

Figure 4: Meshing of solid model in ANSYS.

between the fields. Plane13 is defined by four nodes with up to four degrees of freedom per node. The element has the nonlinear magnetic capability for modelling B-H curves of the material considered. It can be meshed in quadrilateral as well in triangular forms. In this case, the model is meshed in quadrilateral form.

3.3. Meshing. The results in any computational software are highly dependent upon the mesh sizes used for the solution. Since the regenerator area is of interest, fine meshing can be seen at it (Figure 4). It leads to faster convergence rate and relatively less computational time. The validation of mesh size is done by continuously refining the initial guess until there is no appreciable change in the results. At last a mesh size of 0.0005 was found to be optimal.

3.4. Loads. The magnetic loads and thermal loads are explained by Kumar and Shoor [18] in detail along with the magnetic analysis and boundary conditions. The consideration of electrical resistivity leads to Joule heating. Table 2 represents the operating conditions used for simulation.

4. Results and Discussions

The transient analysis of regenerator for 600 s under the magnetic field was performed. The following subsections explain the results of the simulation with and without magnetic fields. A total of 16 cases were analyzed. Due to a large number of models, the images are shown in Appendices A–D (Figures 9–12). The subsequent sections explain the comparative results of different cold end temperature under same magnetic fields (Figures 5–8).

4.1. Temperature Distribution at 0 T. Figure 9(a) shows the temperature distribution at $T_C = 4.2$ K. It is clear that most of the temperature drop happens in the starting part of the regenerator. When the cold end temperature is 6 K (Figure 10(a)), the temperature drops in a similar fashion. However, as seen from Figure 11(a), when the cold end temperature is fixed at 8 K, then 7.13 K was observed to be the lowest temperature in the regenerator. When the cold end is at 10 K, it can be seen in Figure 12(a) that the tip has a higher temperature again. Figure 5 shows the comparison of temperature profiles of the four cases.

At 4.2 K and 6 K the temperature profile is somewhat linear, whereas, for 8 K and 10 K, it is nonlinear. The peak value obtained in the specific heat of Er_3Ni at T_N is the primary reason for this nonlinearity. The ineffectiveness of selected regenerator material above 7.7 K can be seen when only gas-cooling/heating cycle takes place.

Table 2: Operating conditions of regenerator for different magnetic field.

	$B = 0$ T	$B = 1$ T	$B = 3$ T	$B = 4.3$ T
Hot end temperature $T_H = 20$ K	$T_C = 4.2$ K	$T_C = 4.2$ K	$T_C = 4.2$ K	$T_C = 4.2$ K
	$T_C = 6$ K	$T_C = 6$ K	$T_C = 6$ K	$T_C = 6$ K
	$T_C = 8$ K	$T_C = 8$ K	$T_C = 8$ K	$T_C = 8$ K
	$T_C = 10$ K	$T_C = 10$ K	$T_C = 10$ K	$T_C = 10$ K

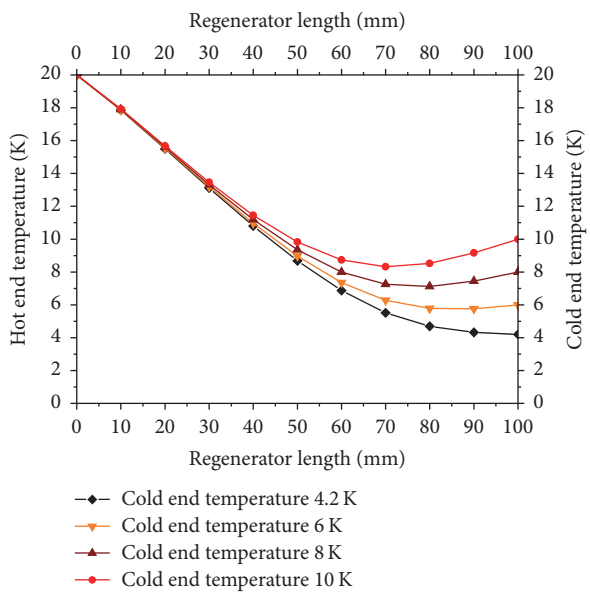

Figure 6: Temperature profile of model at $B = 1$ T.

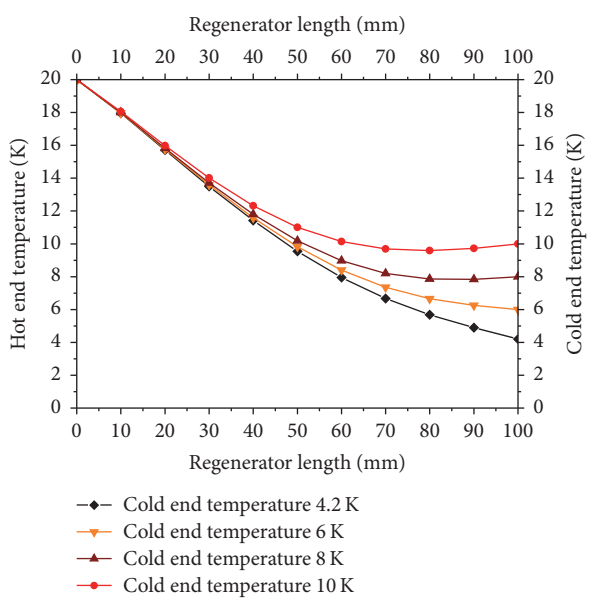

Figure 7: Temperature profile of model at $B = 3$ T.

4.2. Temperature Distribution at $B = 1$ T. Figures 9(b), 10(b), 11(b), and 12(b) show the temperature distribution when T_C is fixed at 4.2 K, 6 K, 8 K, and 10 K, respectively. A similar trend as above is observed in this case also. However, the region of linearity shifts towards 70 mm. It is evident from the comparison of the temperature profiles of the four cases.

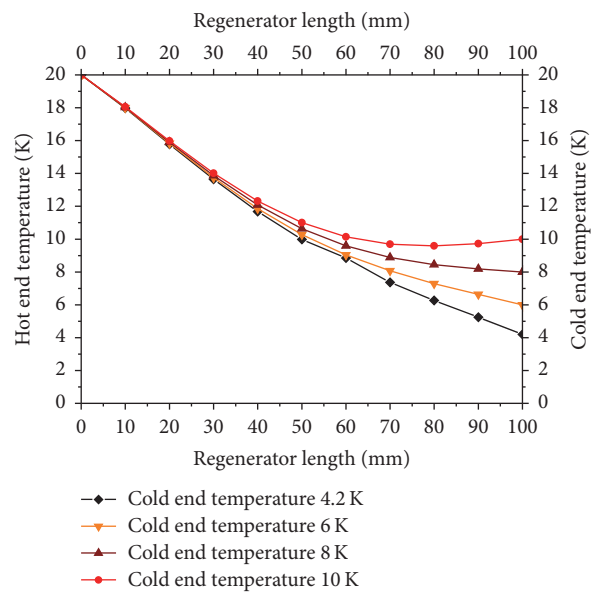

Figure 8: Temperature profile of model at $B = 4.3$ T.

It is evident from Figure 6 that the temperature becomes steeper again after 60 mm for $T_C = 10$ K and 8 K. However, for $T_C = 6$ K and 4 K, the temperature keeps on descending after 70 mm. The effect of Joule heat generation at 1 T affects the temperature profile to a lesser extent as the value is of the order of 10^{-6} [18]. Also it can be seen that the profile has been shifted towards higher side, when compared to case A. The ineffectiveness of selected regenerator material above 7.7 K can be seen when magnetic field is also applied to the model (Figures 9(b) and 12(b)).

4.3. Temperature Distribution at $B = 3$ T. Figures 9(c), 10(c), 11(c), and 12(c) show the temperature distribution for magnetic field 3 T for various T_C. Comparing figures of cold end temperature 8 K and 10 K, it is clearly seen that the temperature is distributed in the regenerator uniformly at 3 T and temperature drop is close to being linear. However, the values are on the slightly higher side than at 0 T and 1 T.

The temperature profile for model 3 at 3 T is presented in Figure 7. For $T_C = 4.2$ K, temperature profile has become somewhat linear. As far as $T_C = 8$ K and 10 K are concerned, after 70 mm the decrease in the specific heat of Er_3Ni causes increase of temperature.

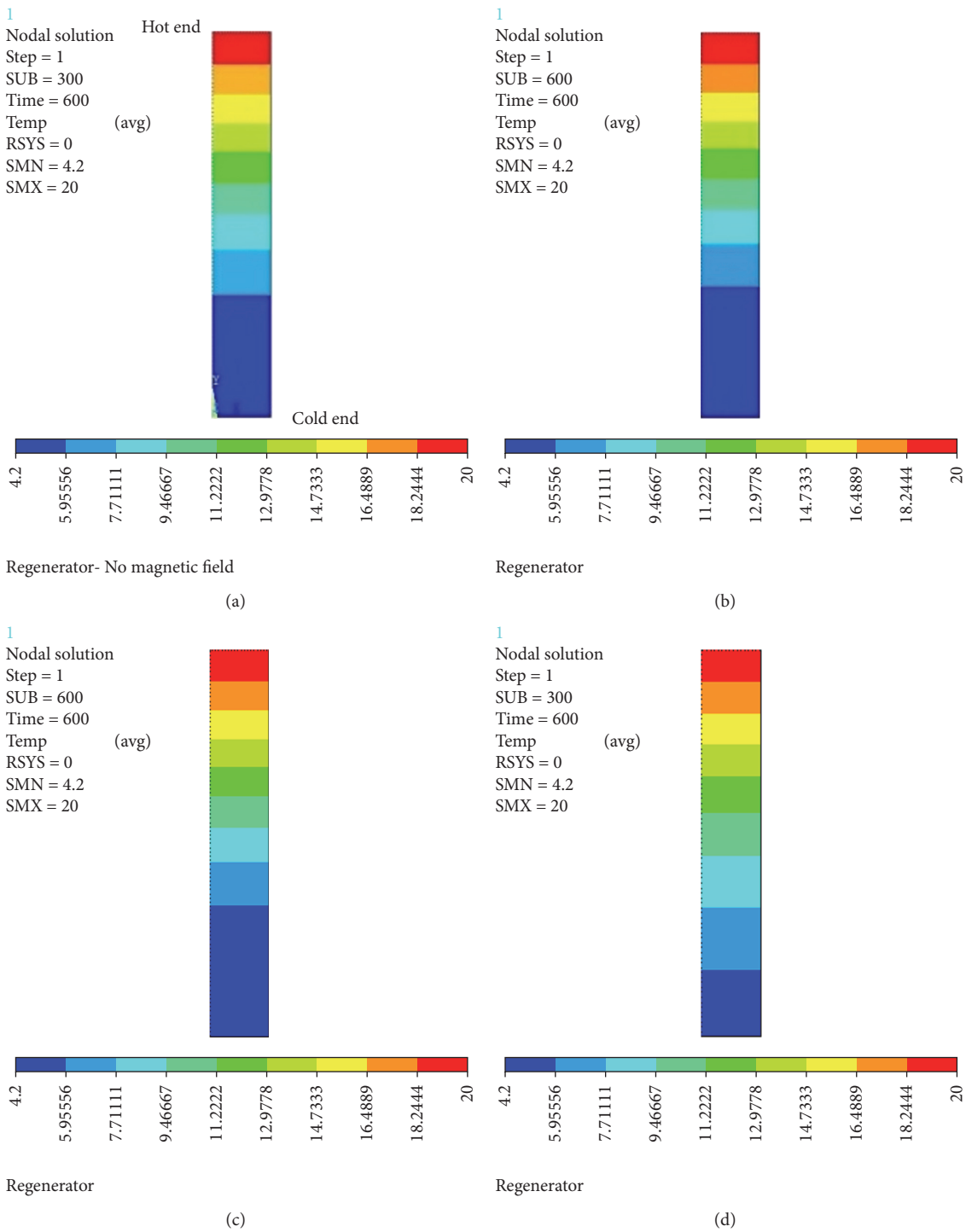

Figure 9: (a) Temperature distribution for 4.2 K at 0 T. (b) Temperature distribution for 4.2 K at 1 T. (c) Temperature distribution for 4.2 K at 3 T. (d) Temperature distribution for 4.2 K at 4.3 T.

4.4. Temperature Distribution at 4.3 T. Figures 9(d), 10(d), 11(d), and 12(d) show the temperature distribution for selected temperatures at 4.3 T. Figure 8 describes the temperature profile at 4.3 T for the model at different cold end temperatures. The trend is similar; however increasing Joule heating shifts the profile towards higher side. The temperature drop is more linear at 4.3 T than at 3 T. The values are on the higher side in this case. Also the graphs show that the temperature drop is more linear at 4.3 T compared to 3 T; however the values are on the higher side at 4.3 T.

The regenerator material has variable heat capacity under different magnetic fields. Therefore at this point, it becomes

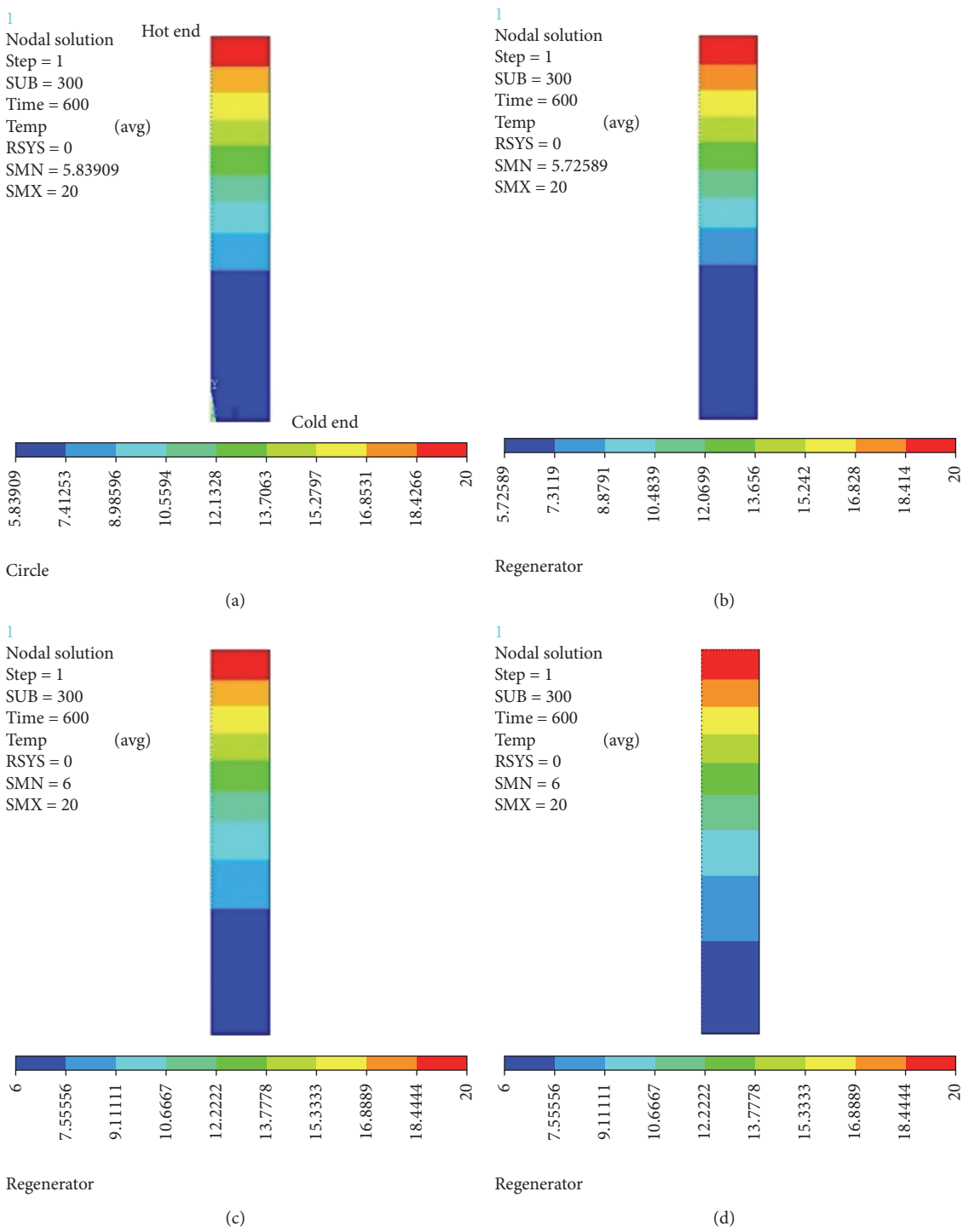

Figure 10: (a) Temperature distribution for 6 K at 0 T. (b) Temperature distribution for 6 K at 1 T. (c) Temperature distribution for 6 K at 3 T. (d) Temperature distribution for 6 K at 4.3 T.

necessary to compare the temperature profiles for same cold end temperature under various magnetic fields. Appendix E shows such comparison at different operating conditions. It is evident from Figures 13(a)–13(d) that the temperature profiles at $B = 0$ T and 1 T closely follow each other in every case. However, the profiles for 8 K and 10 K are on the higher side due to additional thermal load.

Regenerative cryocoolers, in particular, PTCs, are manufactured for a long operating time. Additionally, these devices are designed to produce cooling capacity ~mW [5]. Therefore under high magnetic fields for prolonged period the Joule heat generation comes into play at liquid He temperature (4.2 K). As a result, the additional heat load contributes to the rise in temperature.

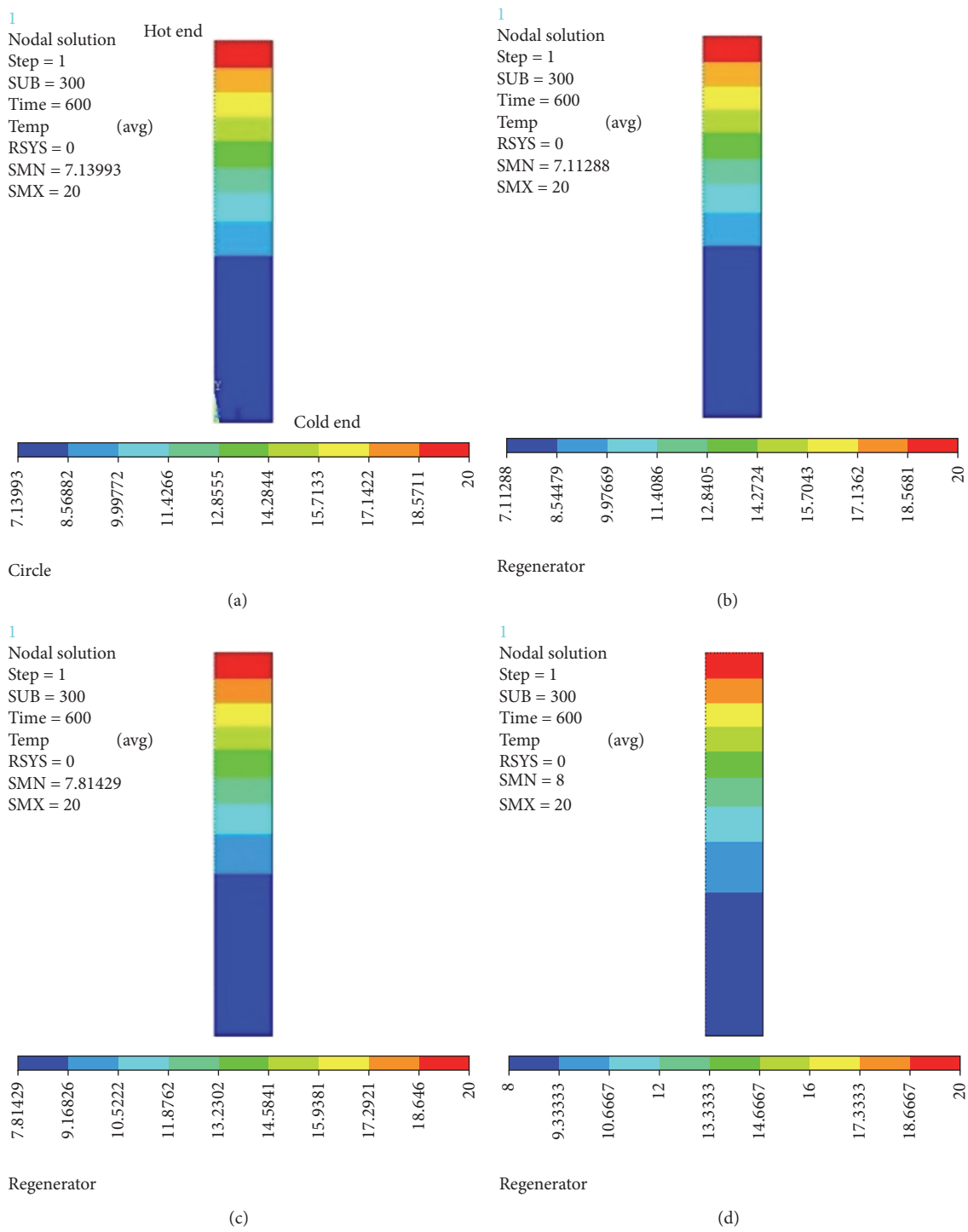

Figure 11: (a) Temperature distribution for 8 K at 0 T. (b) Temperature distribution for 8 K at 1 T. (c) Temperature distribution for 8 K at 3 T. (d) Temperature distribution for 8 K at 4.3 T.

Nowadays more than one material is used in regenerators so as to increase the cooling capacity of the system. Such configuration is known as multilayer regenerators. The cooling capacity is directly related to the effectiveness of the regenerator and in turn the materials used in it. Multilayered regenerators are better to use in comparison to their conventional counterpart. Apparently, in all the above cases the regenerator material becomes ineffective to use above its critical temperature, T_N. Therefore, two different materials with different critical temperatures would provide two peaks in heat capacity for the regenerator bed. For example, $HoCu_2$ with $T_N = 9.8$ K [19] can be used with Er_3Ni

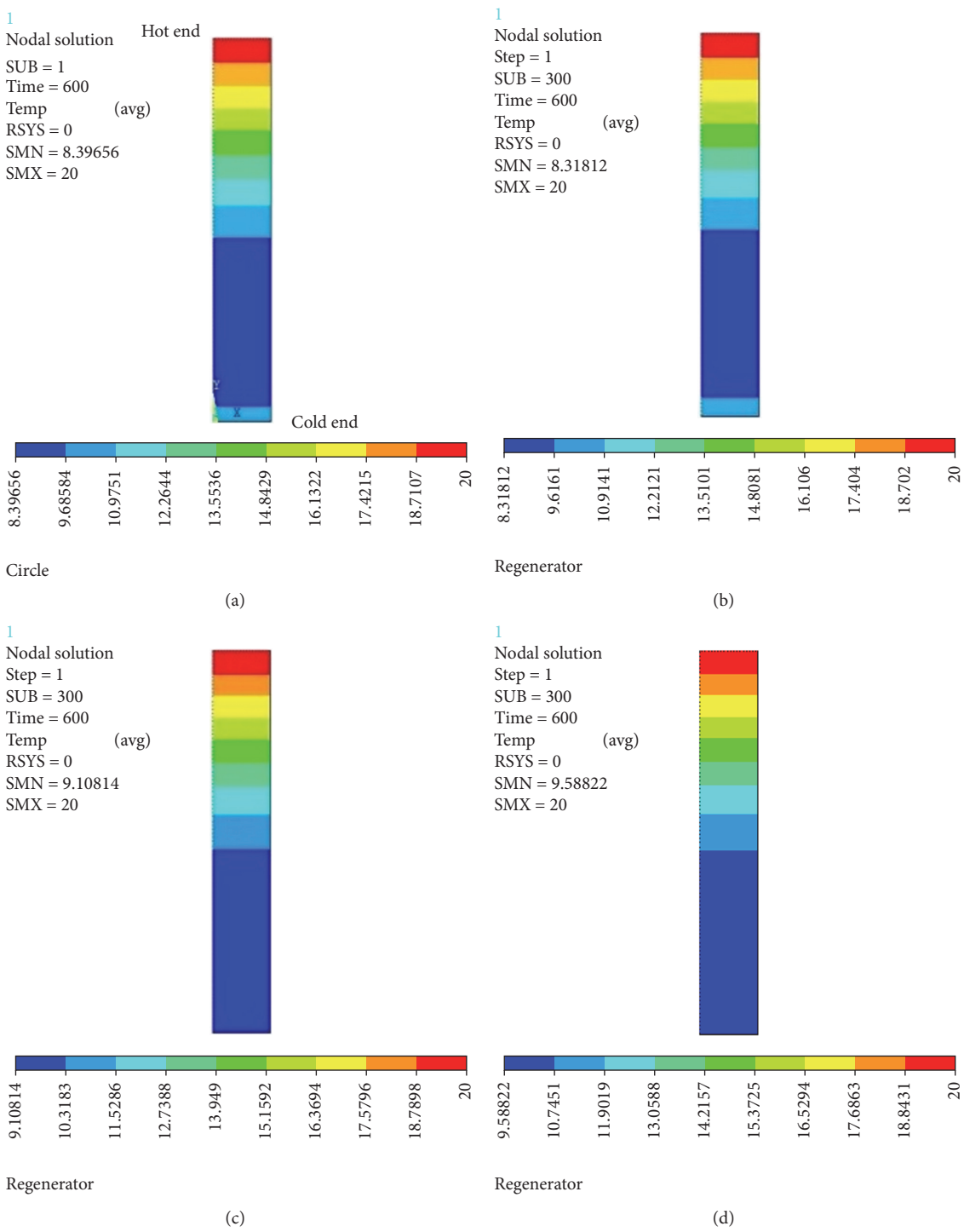

Figure 12: (a) Temperature distribution for 10 K at 0 T. (b) Temperature distribution for 10 K at 1 T. (c) Temperature distribution for 10 K at 3 T. (d) Temperature distribution for 10 K at 4.3 T.

in the regenerator. This kind of configuration can handle wide range of temperatures.

5. Conclusions

In the present work, the effect of magnetic field on cryocooler regenerator is analyzed using FEA package, ANSYS 14.5. Er_3Ni is selected as matrix material. In addition to the thermal and magnetic properties, the electrical resistivity is also considered to account for Joule heating. A total of 16 cases were simulated and compared. At the end the following points can be concluded:

(1) The specific heat of Er_3Ni is crucial as regenerator material, and above its Néel temperature, it is

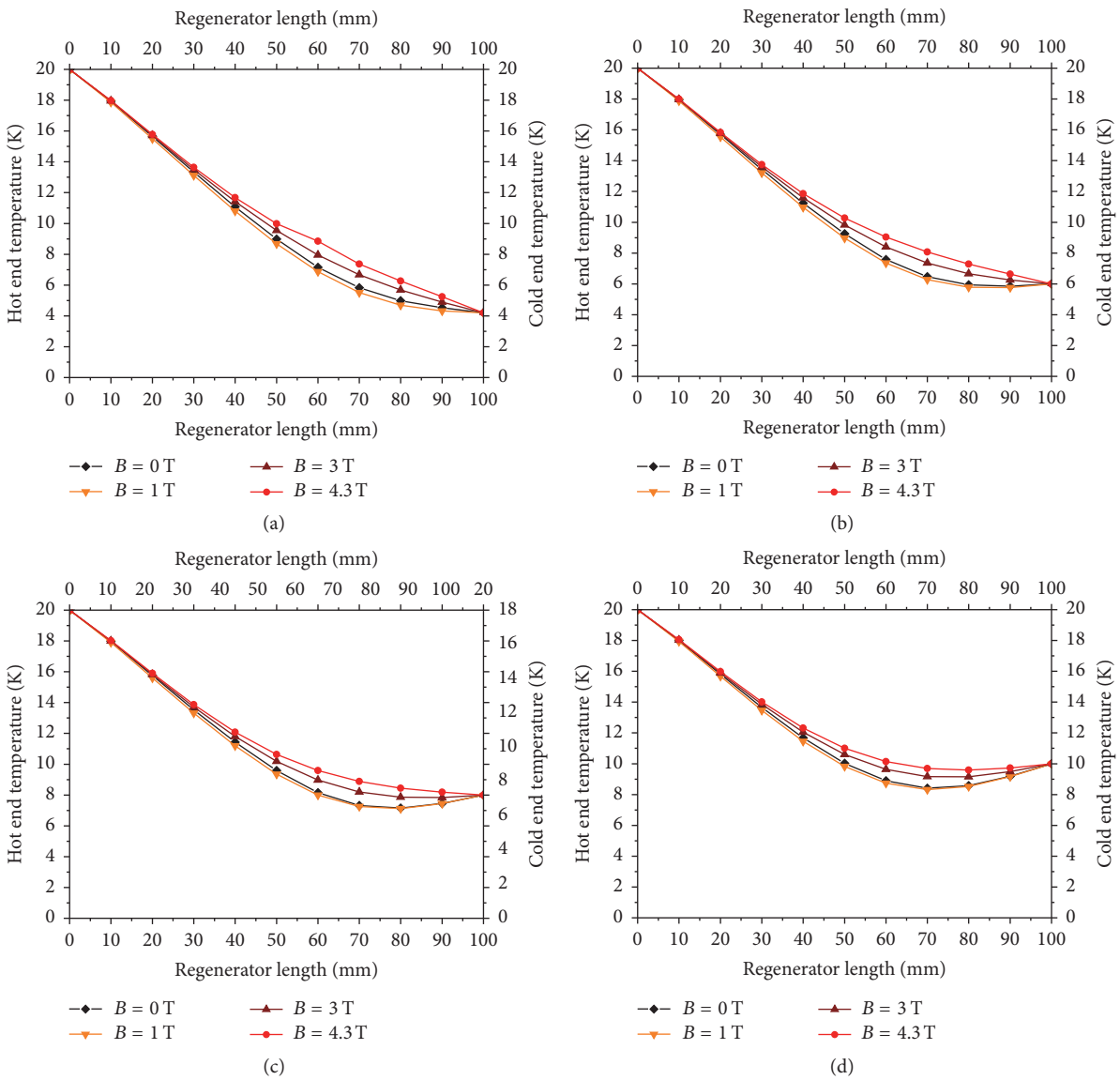

Figure 13: (a) Temperature profile at $T_C = 4.2$ K. (b) Temperature profile at $T_C = 6$ K. (c) Temperature profile at $T_C = 8$ K. (d) Temperature profile at $T_C = 10$ K.

ineffective to use since the temperature shifts towards higher side.

(2) The consideration of the influence of magnetic field upon the specific heat of Er_3Ni shows that up to 1 T the regenerator would work satisfactorily. However, for higher magnetic fields the performance would degrade. The patterns observed in the heat capacity of Er_3Ni at different temperatures and magnetic fields are the reason behind this.

(3) The model also explains that multilayered regenerators are better to use and the material interface should be at the place where temperature profile shifts towards higher side. At the interface, the temperature would not shift towards higher side. The reason is attributed to the peak in specific heat capacity at the critical temperature of the second material used. As stated above, $HoCu_2$ is better to use at 10 K and Er_3Ni is better to use at 6 K and 4.2 K. Therefore, both can be constituted together and that regenerator would work efficiently from 10 K to 4.2 K.

Appendix

A. Temperature Distribution for $T_C = 4.2$ K from ANSYS 14.5

See Figure 9.

B. Temperature Distribution at $T_C = 6$ K from ANSYS 14.5

See Figure 10.

C. Temperature Distribution at $T_C = 8$ K from ANSYS 14.5

See Figure 11.

D. Temperature Distribution at $T_C = 10$ K from ANSYS 14.5

See Figure 12.

E. Comparison of the Same T_C for $B = 0$ T, 1 T, 3 T, and 4.3 T

See Figure 13.

Competing Interests

The authors declare that they have no competing interests.

Acknowledgments

The authors are thankful to Ms. Narinder Chumber for her constant support throughout the work and valuable suggestions in preparing the manuscript.

References

[1] G. Walker, *Cryocoolers*, The International Cryogenics Monograph Series, Springer, Berlin, Germany, 1st edition, 1983.

[2] R. Radebaugh, "Cryocoolers: the state of the art and recent developments," *Journal of Physics: Condensed Matter*, vol. 21, no. 16, Article ID 164219, 2009.

[3] T. Kuriyama, R. Hakamada, H. Nakagome et al., "High efficient two-stage gm refrigerator with magnetic material in the liquid helium temperature region," in *Advances in Cryogenic Engineering*, R. W. Fast, Ed., vol. 35 of *Advances in Cryogenic Engineering*, pp. 1261–1269, Springer, Boston, Mass, USA, 1990.

[4] T. Hashimoto, M. Ogawa, A. Hayashi, M. Makino, R. Li, and K. Aoki, "Recent progress on rare earth magnetic regenerator materials," in *Advances in Cryogenic Engineering*, pp. 859–865, Springer, New York, NY, USA, 1991.

[5] Y. Matsubara and J. L. Gao, "Novel configuration of three-stage pulse tube refrigerator for temperatures below 4 K," *Cryogenics*, vol. 34, no. 4, pp. 259–262, 1994.

[6] J. L. Gao, Y. Hiresaki, and Y. Matsubara, "A hybrid two-stage refrigerator operated at temperatures below 4K," in *Advances in Cryogenic Engineering: Part A*, P. Kittel, Ed., vol. 41 of *A Cryogenic Engineering Conference Publication*, pp. 1495–1502, Springer, Berlin, Germany, 1996.

[7] K. Gschneidner, A. Pecharsky, and V. Pecharsky, "Low temperature cryocooler regenerator materials," *Cryocoolers*, vol. 12, pp. 457–465, 2002.

[8] K. A. Gschneidner Jr., A. O. Pecharsky, and V. K. Pecharsky, "Development of new cryocooler regenerator materials—ductile intermetallic compounds," in *Cryocoolers 13*, pp. 363–371, Springer, New York, NY, USA, 2005.

[9] K. A. Gschneidner, A. O. Pecharsky, L. Hale, and V. K. Pecharsky, "Low temperatureproperties of some er-rich tntermetulic compounds," in *Proceedings of the Advances in Cryogenic Engineering: Transactions of the International Cryogenic Materials Conference*, vol. 711 of *AIP Conference Proceedings*, Anchorage, Ala, USA, June 2004.

[10] Y. Spichkin and A. M. Tishin, "The magnetocaloric effect and its applications," *Materials Today* , vol. 6, no. 11, p. 51, 2003.

[11] C. Bécle, R. Lemaire, and D. Paccard, "Experimental evidence for anisotropic interactions in some rare-earth intermetallic compounds," *Journal of Applied Physics*, vol. 41, no. 3, pp. 855–863, 1970.

[12] S. Fujimoto, K. Kazami, Y. Takada, T. Yoshida, H. Ogata, and H. Kado, "Cooling of SQUIDs using a Gifford-McMahon cryocooler containing magnetic regenerative material to measure biomagnetism," *Cryogenics*, vol. 35, no. 2, pp. 143–148, 1995.

[13] E. Talik, "Magnetic and transport properties of the R_3Ni system (R = Y, Gd, Tb, Dy, Ho, Er)," *Physica B: Condensed Matter*, vol. 193, no. 3-4, pp. 213–220, 1994.

[14] K. H. J. Buschow, "Intermetallic compounds of rare-earth and 3d transition metals," *Reports on Progress in Physics*, vol. 40, no. 10, pp. 1179–1256, 1977.

[15] M. Ogawa, R. Li, and T. Hashimoto, "Thermal conductivities of magnetic intermetallic compounds for cryogenic regenerator," *Cryogenics*, vol. 31, no. 6, pp. 405–410, 1991.

[16] Y. Tokai, A. Takahashi, M. Sahashi, T. Hashimoto, H. Yayama, and A. Tomokiyo, "Magnetic field influence on Er_3Ni specific heat," *Japanese Journal of Applied Physics*, vol. 31, no. 10, pp. 3332–3335, 1992.

[17] ANSYS Inc, "ANSYS mechanical APDL element reference," in *ANSYS Manual, Release 14.5*, vol. 15317, pp. 1377–1390, 2012, http://www.ansys.com.

[18] R. Kumar and S. Shoor, "Finite element analysis of magnetic field effect on cryocooler regenerators," *International Journal of Research in Science & Technology*, vol. 6, no. 4, pp. 15–29, 2016.

[19] Y. Hashimoto, H. Fujii, H. Fujiwara, and T. Okamoto, "Magnetic properties of rare earth copper intermetallic compounds, RCu_2. I. heavy rare earth," *Journal of the Physical Society of Japan*, vol. 47, no. 1, pp. 67–72, 1979.